# Adhesion energy in carbon nanotube-polyethylene composite: Effect of chirality

M. Al-Haik and M. Y. Hussaini[a)]
*School of Computational Science and Information Technology, Florida State University, Tallahassee, Florida 32306-4120*

H. Garmestani
*School of Materials Science and Engineering, Georgia Institute of Technology, Atlanta, Georgia 30332*

(Received 24 June 2004; accepted 12 January 2005; published online 23 March 2005)

This work presents a study of the adhesion energy between carbon nanotube-polyethylene matrix based on molecular dynamics simulations. Specifically, the study focuses on the influence of carbon nanotube chirality on adhesion energy. It is observed that composites that utilize nanotubes with smaller chiral angles achieve higher adhesion energy, and tend to have smaller diameter and longer cylindrical axes compared to those with larger chiral angles. A zigzag nanotube (zero-chiral angle) undergoes considerable deformation to achieve an equilibrium configuration that has relatively maximum adhesion energy. On the other hand, the armchair nanotube (30° chiral angle) deforms moderately to reach equilibrium with minimal adhesion bonds to the polyethylene matrix. © *2005 American Institute of Physics*. [DOI: 10.1063/1.1868060]

## I. INTRODUCTION

Since their initial discovery in 1991 by Iijima,[1] carbon nanotubes (CNTs) have attracted a good deal of interest because of their unique optical, electronic, and mechanical properties. Many researchers have reported mechanical properties of CNT that exceed those of existing materials. For example, theoretical and experimental investigations[2,3] have shown that CNTs have remarkable mechanical properties with Young's modulus and tensile strength as high as 1 TPa and 200 GPa, respectively. Owing to their exceptional mechanical properties, high aspect ratio, and low density, CNTs are promising reinforcements for polymer composites.[4]

The effective utilization of CNTs in composite applications depends strongly on the ability to disperse the nanotubes homogeneously throughout the polymer matrix without destroying the integrity of the nanotubes. In earlier investigations,[5,6] the authors have employed high magnetic fields to disperse CNTs in a polymeric matrix while maintaining their structural integrity. Besides homogeneous dispersion good interfacial bonding is required to achieve load transfer across the CNT-polymer interface.[7]

Due to difficulties in devising experiments to study the CNT-polymer interface, molecular dynamics (MD) simulations have become increasingly popular in the investigations of reinforcement mechanisms in CNT-polymer composite systems. MD simulations of nanocomposite systems were investigated by Wei *et al.*,[8] Liao and Li,[9] Frankland *et al.*,[10] and Frankland and Harik,[11] to cite a few.

Wei *et al.*[8] studied the chemical bonding between the polymer and CNT using the Tersoff–Brenner potential. They found that multiple-site chemical bonding was energetically favorable, i.e., it enhanced the mechanical load transfer from the polymer chain to the CNT. In the absence of chemical bonding, Liao and Li[9] observed that for a single-wall CNT(SWCNT)-polystyrene (PS) composite system, the interfacial adhesion forces stem from the electrostatic and van der Waal interactions, the radial deformation induced by these forces, and the mismatch in the coefficients of thermal expansion for the polymer and the SWCNT. They found that the interfacial shear stress of the CNT-PS system (due to CNT pullout) is significantly higher than most carbon fiber reinforced composite systems. Their MD simulations used MM+ force field and Lennard-Jones potential. Their composite model consisted of only 4000 atoms and a 2 nm long armchair CNT, together with random coils of PS (2–80 monomers). Frankland *et al.*[10] considered a CNT-polyethylene composite system, which contained a 6 nm long CNT (880 carbon atoms) and 178 chains of 42-methylene monomer. Their MD simulation modeled the nonbonded interactions using Lennard-Jones potential, and about 23 000 atoms. Their key conclusion was that the interfacial shear strengths and critical lengths required for load transfer could be enhanced by an order of magnitude with the formation of cross links involving less than 1% of the nanotube carbon atoms. More recently, Frankland and Harik[11] carried out MD simulations with a Lennard-Jones potential, which captured the full nanotube pull out process. They found a linear relation between interfacial forces and velocity, and estimated an effective viscosity for the interfacial friction model.

While most of the cited literature considered MD simulations for nanotubes of different lengths with different types of polymers, there has been no MD simulation that investigates the effect of nanotube chirality on the adhesion properties. It is the focus of the present study. Assuming that there is no chemical bonding between the CNT and the polyethylene matrix after mixing, the system can be investigated for nonbonded interactions constituting the adhesion energy. This assumption was validated experimentally by Chang *et*

[a)]Electronic mail: myh@csit.fsu.edu

 

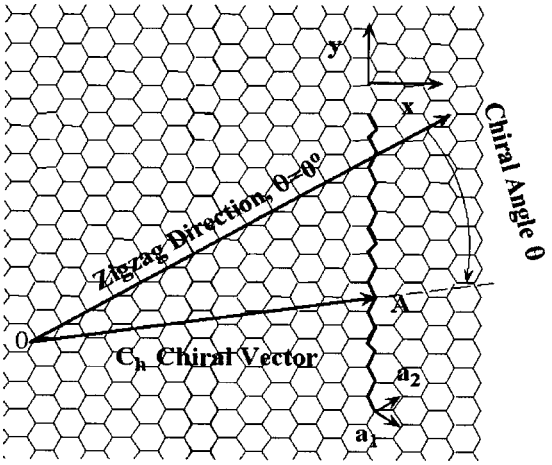


FIG. 1. Definition of chiral angle in terms of chiral vector and zigzag direction.

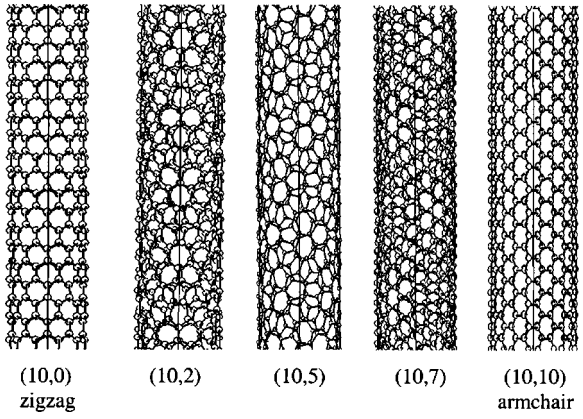


FIG. 2. Schematics of five different chiral nanotubes.

*al.*,[12] for a system of CNT and polypyrole matrix using Raman scattering and x-ray diffraction. The adhesive energy is computed as the difference between the total potential energy of the composite material and the sum of the individual potential energies of the constituents in isolation.

The chirality, defined by the chiral vector $\mathbf{C}_h$ and the chiral angle $\theta$ (briefly described here for completeness), characterizes the atomic structure of a nanotube. They are also called the roll-up vector (that defines its diameter) and the helical angle, respectively. The chiral vector, $\mathbf{C}_h = n\mathbf{a}_1 + m\mathbf{a}_2$, is defined on the honeycomb lattice of carbon atoms by unit vectors $\mathbf{a}_1$ and $\mathbf{a}_2$ (shown in Fig. 1), and the integers $(n,m)$ which represent the number of steps along the zigzag carbon bonds of the hexagonal lattice. The chiral angle is the smallest angle enclosed by the nanotube axis and the row of edge-sharing hexagons, or, in other words, the smallest angle between the circumference line (chiral vector) and the primitive lattice vector (zigzag direction) on the hexagonal sheet as shown in Fig. 1. SWCNTs can be visualized as the sheet of graphite, marked by bold lines in Fig. 1, rolled into a tube such that the tip of the chiral vector touches its tail. The nanotube configurations where the chiral angles assume the extreme values of 0° and 30° are the limiting cases referred to as "zigzag" and "armchair", respectively. In terms of the chiral vector, the zigzag nanotube is defined as $(n,0)$ and the armchair nanotube as $(n,n)$, respectively. The chiral angle $\theta$ may be viewed as a measure of the twist in the tube, and this chirality has a significant influence on the nanotube diameter.

The thermal,[13] electronic,[14] and mechanical[15] properties of CNT vary substantially depending on the CNT diameters and chiral angles. In this work, we focus on the effect of chirality on the adhesion energy between a SWCNT and a polyethylene matrix.

## II. COMPUTATIONAL EXPERIMENT

In this study, the initial atomic configurations of CNT are obtained by creating the planar hexagonal carbon atom network corresponding to an $(n,m)$ nanotube cut open axially. The nearest-neighbor distance between carbon atoms are set to 0.142 nm. This plane is then mapped onto a cylindrical surface to form a tube. Five types of CNTs, with different chirality ranging between zigzag (10,0) and armchair (10,10) are generated as shown in Fig. 2. The corresponding chiral angle $\theta$ and diameter $D_n$ of a SWCNT with $(n,m)$ indices could be determined by using the rolling graphene model:[16]

$$\theta = \arctan\left(\frac{\sqrt{3}m}{2n+m}\right), \quad D_n = \frac{\sqrt{3}}{\pi} b\sqrt{(n^2+m^2+nm)}, \quad (0 \leqslant m \leqslant n), \tag{1}$$

where $b$ is the C–C bond length (0.142 nm). While these nanotubes have different diameters and lengths, they all consist of 600 carbon atoms each. By analyzing the C–C bonding mode along the tube, we notice a significant difference between the behavior of atoms located at the ends and those at the body. The number of the nearest neighbors (only two) at the mouth ends is less than that for the body atom (three), and carbon atoms at the mouth are unsaturated. The unsaturated boundary effect is avoided by adding hydrogen atoms at the ends of the CNTs.[17,18] The exact numbers of carbon and hydrogen atoms for each chiral nanotube are presented in Table I. The polymeric matrix consists of amorphous random chains of 300 methylene monomers (-C–H2-). The atomic force field used here is the MM3 potential that is comprised of bond stretching, angle bending, stretch bend, angle angle, out-of-plane bend, torsional angle potentials, and a nonbonded (12-6) Lennard-Jones potential. MM3 was parameterized, tested, and validated for hydrocarbons.[19,20] The choice of MM3 for this investigation was based on its reliability to capture the constitutive behavior of CNTs and their composites as documented by several investigators.[21–24]

We start by equilibrating the individual reference systems of polyethylene and nanotubes. First, we employ a limited memory BFGS method[25] in order to relax the initial configurations of the polyethylene and the CNT to their local potential energy minimum. The potential energy is a function of the positions of N atoms and is given by[19,27]

TABLE I. Total number of atoms utilized in MD simulation for chiral nanotubes (NTs) and polyethylene matrix.

| | H atoms | C atoms | Nanotube diameter (nm) | Nanotube length (nm) | Chiral angle $\theta°$ |
|---|---|---|---|---|---|
| Polyethylene | 602 | 300 | ⋯ | ⋯ | ⋯ |
| (10,0) NT zigzag | 40 | 600 | 0.783 | 6.5541 | 0.00 |
| (10,2) NT | 43 | 600 | 0.934 | 6.0611 | 8.95 |
| (10,5) NT | 50 | 600 | 1.036 | 5.2281 | 19.11 |
| (10,7) NT | 54 | 600 | 1.158 | 4.8061 | 24.18 |
| (10,10) NT armchair | 60 | 600 | 1.356 | 4.1278 | 30.00 |

$$E(r_1,r_2,\ldots,r_N)=\sum_{i=1}^{N-1}\sum_{j>i}^{N}E_{2\_\mathrm{body}}(i,j,|r_i-r_j|)+\sum_{i=1}^{N-2}\sum_{j>i}^{N-1}\sum_{k>j}^{N}E_{3\mathrm{-body}}(i,j,k,r_i,r_j,r_k)+\sum_{i=1}^{N-3}\sum_{j>i}^{N-2}\sum_{k>j}^{N-1}\sum_{n>k}^{N}E_{4\mathrm{-body}}(i,j,k,n,r_i,r_j,r_k,r_n)+\sum_{i=1}^{N}\sum_{j=i+1}^{N}4\varepsilon_{ij}\left[\left(\frac{\sigma_{ij}}{r_{ij}}\right)^{12}-\left(\frac{\sigma_{ij}}{r_{ij}}\right)^{6}\right]+\sum_{i=1}^{N}\sum_{j=i+1}^{N}\frac{q_iq_j}{4\pi\varepsilon_0 r_{ij}}, \tag{2}$$

where $E_{2\mathrm{-body}}$ is a two-body potential between two atoms (bond stretching and torsion stretch interaction), $E_{3\mathrm{-body}}$ is the potential between three atoms (angle bending, stretch-bend, and bend-bend interactions), and $E_{4\text{-body}}$ is the potential between four atoms (bond torsion). The last two terms in Eq. (2) are, respectively, the van der Waals nonbonding interactions and electrostatic interactions between all pairs of atoms ($i$ and $j$) that are in different molecules, or that are in the same molecule but separated by at least three bonds. The initial dimensions of the boundary box for the polyethylene monomers are $8.63\times3.64\times2.27$ nm. The polyethylene cell is relaxed through the minimization of the potential energy to a convergence criterion where the root-mean-square (rms) atom force cutoff of the energy is 0.0001 kcal/mol Å. The final dimensions of the relaxed polyethylene cell are $5.0\times2.0\times2.94$ nm. The final density of polyethylene upon equilibration is (0.70 g/cm$^3$). The potential energy for each chiral nanotube was minimized via LM-BFGS in a similar manner. The initial dimensions of the armchair nanotube cell were $4.58\times2.68\times3.51$ nm and the dimensions of the relaxed nanotube were $4.06\times1.67\times2.90$ nm.

Upon achieving the state of minimum potential energy for nanotubes and polyethylene individually (Fig. 3), we start by moving the (10,10) CNT cell very close to the relaxed cell of polyethylene. The overall dimensions of the bounding box for the composite system (polyethylene and armchair nanotube) are approximately $5.25\times2.87\times3.59$ nm, such that the closest distance between the outer surface of nanotube and the nearest methylene monomer is 0.5 nm. The cell is tested to ensure there are no overlapping positions between the nanotube and polyethylene atoms. LM-BFGS is employed once more for each composite system so that the MD simulation starts from a minimal potential energy configuration. These procedures were repeated for the other four different nanotubes using different simulation box dimensions to accommodate different lengths of the corresponding nanotubes. Periodic boundary conditions were used for all simulations.

The composite connected state is obtained by equilibrating the system after connecting the nanotube with the polymeric matrix. This equilibration is conducted by using the Newton's equation of motion;

$$F_i=m_i\frac{d^2r_i}{dt^2}=-\partial\frac{E(r_1,r_2,\ldots,r_N)}{\partial r_i}, \tag{3}$$

where $m_i$ is the atomic mass of the $i$th atom. Successive configurations of the system are generated by the time integration of Eq. (3). The result is a trajectory that specifies how the positions and velocities of the particles in the system vary with time. A statistical ensemble is used to compute the average of the physical quantity of interest. The physical quantity is taken as the time average on the trajectory. Statistical mechanics relates MD averages to their thermodynamics counterparts, and the ergodic hypothesis can be invoked to justify equating trajectory averages to ensemble-based thermodynamic properties.[26,27] For each composite system, we conduct a MD simulation for 10 ps, with a time step of 1.0 fs under constant temperature of 300 K and external pressure of 1.0 atm.

All of the MD simulations are performed within the framework of the *NPT* (Isothermal-isobaric) statistical ensemble[28] for a periodic system, which is characterized by a

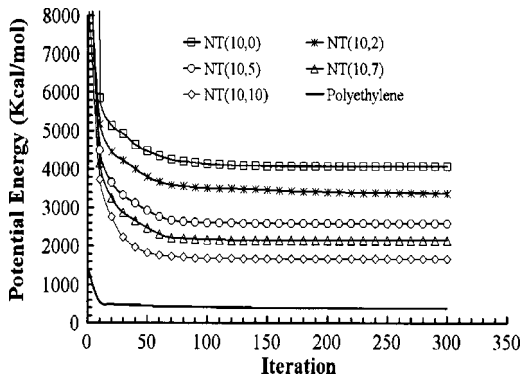


FIG. 3. Minimum potential energy configuration for the individual members of the composites; minimization based on LM-BFGS algorithm with rms 0.0001 kcal/mol. Å convergence.

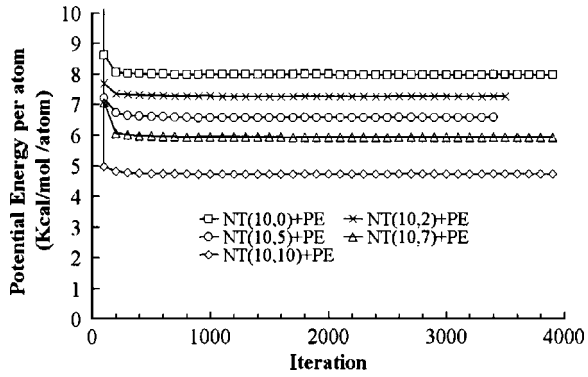


FIG. 4. Minimum potential energy per atom for the nanotube based composites; Minimization based on LM-BFGS algorithm with rms 0.0001 kcal/mol. Å convergence.

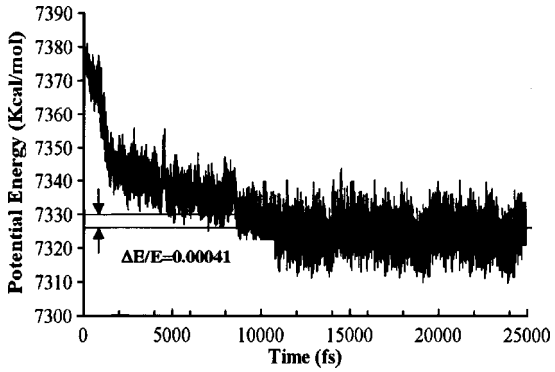


FIG. 5. Potential energy evolution for armchair nanotube polyethylene composite during 25 ps of MD simulation using *NPT* ensemble.

fixed number of atoms, *N*, a fixed pressure, *P*, and a fixed temperature, *T*. The *NPT* ensemble is an attractive choice. First, it allows, the MD simulation for systems with a relatively small number of particles (1000 atom)[29] by calculating the trajectories in various ways. Second, the *NPT* ensemble simulates the effect of surrounding particles without creating undesirable surfaces. Third, this method simulates both the forces that drive the system to equilibrium at a given temperature and pressure and the forces that cause the energy and volume of the system to fluctuate about their equilibrium values.[22] A Nose–Hoover extended system thermostat[30] is used for the temperature control, and the Berendsen[31] method is used to maintain a constant desired pressure in the periodic box. The numerical integration of the equation of motion is performed using the velocity Verlet algorithm.[32] The integration time step is 1.0 fs, and the cutoff distance for the 12-6 Lennard-Jones potential is 1.05 nm. The simulations are repeated using the minimum energy configuration of the other chiral nanotubes with the polyethylene matrix. For all the MD simulations, the initial distance between the nanotube and the polyethylene was set to 0.5 nm. The simulations are carried out using TINKER©; a package of molecular simulation subroutines.[33,34]

## III. RESULTS AND DISCUSSION

Plotted in Fig. 4 are the minimum potential energies per atom for the relaxed systems of the nanocomposites achieved through the LM-BFGS minimization algorithm. The chirality seems to influence the change in the potential energy for the different nanocomposite systems. As the chirality indices (chiral angle) increase, the potential energy decreases. For example, the potential energy of the armchair nanotube polyethylene composite is 40% less than that for the zigzag nanotube-based composite.

The relaxed nanocomposite systems were further equilibrated by conducting MD simulation. The evolution of the potential energy for the armchair nanotube composite system is shown in Fig. 5.

The change in the potential energy from 10 to 25 ps is observed to be 0.04% of the potential energy at 10 ps. The relation between the approximation inherent in the integration algorithm and the fluctuation in potential energy is discussed by Leach[27] (p. 359), where he indicates that a variation of the potential energy in the orange 0.0001–0.001 is generally considered acceptable as an equilibrium criterion. Since the change in potential energy between 10 and 25 ps period is found to be about 0.00041, the system could be reasonably assumed to have reached equilibrium. Therefore, in the interest of computational time, the simulations are terminated at 10 ps.

The adhesion energy is estimated as the difference between the potential energy of the composite system and the potential energies for the polyethylene and the corresponding CNT: $\Delta E = E_{\text{Total}} - (E_{\text{CNT}} + E_{\text{PE}})$ where $E_{\text{Total}}$ is the total potential energy of the composite at the end of equilibration, $E_{\text{CNT}}$ is the energy of the nanotube alone, and $E_{\text{PE}}$ is the energy of the polymer alone. Both $E_{\text{CNT}}$ and $E_{\text{PE}}$ were precalculated via separate MD simulation as well. Figure 6 depicts the adhesion energy per atom of the composite versus the corresponding chirality of the nanotube. It is clear that the adhesion energy attains the highest value for the zigzag system, while the armchair nanotube composite produces the least adhesion energy system. This can be attributed to the effect of chirality of the nanotube on its length and diameter. Nanotubes with low chirality indices tend to have smaller diameter and longer cylindrical axes compared to those with high chirality, such as the armchair nanotube (10,10). The correlation between the diameter of the nanotubes and the potential energy as obtained via MD simulation is in good

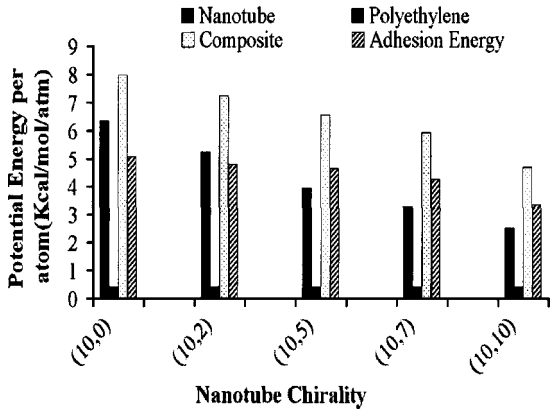


FIG. 6. Adhesion energy between different chiral nanotubes and polyethylene chains on per atom basis.

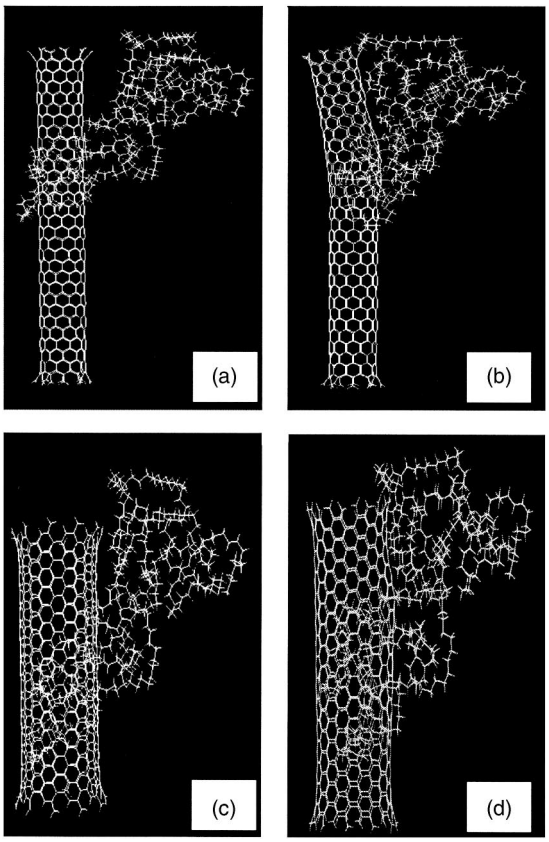


FIG. 7. Instantaneous trajectory for the zigzag (10,0) based composite at (a) 0 ps and (b) 10 ps. The trajectory of the armchair (10,10) based composite at (c) 0 ps and (d) 10 ps. Velocity form of Verlet algorithm was used to integrate the equation of motion. *NPT* ensemble was utilized through all the MD simulations.

agreement with that obtained by classical elasticity theory, where the total energies are inversely preoperational to the square of the radius.[35] Therefore, the adhesion energy between the CNT and the polymer strongly depends on the diameter of CNT.

The longer the nanotube, the more sites exist to form bonds between the nanotube and polyethylene matrix. This can be verified by plotting the trajectories of the composites before and after the MD equilibrating process. Figure 7 shows the initial and final instants in the evolution of the trajectories for the zigzag and the armchair based composites. It is clear from Figs. 7(a) and 7(b) that the zigzag nanotube undergoes considerable deformation to achieve a configuration of minimum adhesion energy. On the other hand, the armchair nanotube, Figs. 7(c) and 7(d), deforms moderately to establish adhesion bonds to the polyethylene matrix.

## IV. CONCLUSIONS

In this work, we used classical MD with an MM3 force field to study the adhesion energy of SWCNTs of various chiralities embedded in a polyethylene matrix. Substantial adhesion exists between the nanotube and the polyethylene when the nanotube has a low chiral indices or smaller chiral angle (relatively long). This observation is in good agreement with the composite principle that a high aspect ratio of the fiber yields stronger adhesion with the matrix. Since there is currently no simple way to measure the critical length of SWCNTs, the current investigation gives an idea of what might be a better configuration of the CNT-polyethylene interaction to ensure better adhesion.

For many nanostructured materials, the trade-off between structure and property must be established before the material can be optimized for a given application. The method presented in this article provides a means for parametrically exploring these structure-property relationships.

[1]S. Iijima, Nature (London) **354**, 56 (1991).
[2]M. F. Yu, B. S. Files, S. Arepalli, and R. Ruff, Phys. Rev. Lett. **84**, 5552 (2000).
[3]C. Bower, R. Rosen, L. Jin, J. Han, and O. Zhoua, Appl. Phys. Lett. **74**, 3317 (1999).
[4]V. Lordi and N. Yao, J. Mater. Res. **15**, 2770 (2002).
[5]E. S. Choi, J. S. Brooks, D. L. Eaton, M. S. Al-Haik, M. Y. Hussaini, H. Garmestani, D. Li, and K. Dahmen, J. Appl. Phys. **94**, 6034 (2003).
[6]H. Garmestani, M. S. Al-Haik, D. Li, R. Tanannbaum, K. Dahmen, S. S. Sablin, and M. Y. Hussaini, Adv. Mater. (Weinheim, Ger.) **15**, 1918 (2003).
[7]D. Qian, E. C. Dickey, R. Andrews, and T. Rantell, Appl. Phys. Lett. **6**, 2868 (2000).
[8]C. Wei and K. Cho, *Proceedings of the MRS Spring Meeting* (Materials Research Society, Pittsburgh, 2001).
[9]K. Liao and S. Li, Appl. Phys. Lett. **79**, 4225 (2001).
[10]S. J. V. Frankland, A. Caglar, D. W. Brenner, and M. Griebel, J. Phys. Chem. B **106**, 3046 (2002).
[11]S. J. V. Frankland and V. M. Harik, Surf. Sci. **525**, L103 (2003).
[12]B. H. Chang, Z. Q. Liu, L. F. Sun, D. S. Tang, W. Y. Zhou, G. Wang, L. X. Qian, S. S. Xie, J. H. Fen, and M. X. Wan, J. Low Temp. Phys. **119**, 41 (2000).
[13]S. Y. Mensah, F. K. A. Allotey, N. G. Mensah, and G. Nkrumah, J. Phys.: Condens. Matter **13**, 5653 (2001).
[14]S. D. Liang and N. S. Xu, Appl. Phys. Lett. **83**, 1213 (2003).
[15]T. Natsuki, K. Tantrakarn, and M. Endo, Carbon **42**, 39 (2004).
[16]M. S. Dresselhaus, G. Dresselhaus, and R. Saito, Carbon **33**, 883 (1995).
[17]G. Zhou, W. Duan, and B. Gu, Phys. Rev. Lett. **87**, 095504 (2001)
[18]C. W. Chen and M. H. Lee, Nanotechnology **15**, 480 (2004).
[19]N. L. Allinger, Y. H. Yuh, and J. H. Lii, J. Am. Chem. Soc. **111**, 8551 (1989).
[20]N. L. Allinger, F. Li, L. Yan, and J. C. Tai, J. Comput. Chem. **11**, 868 (1990).
[21]G. M. Odegard, T. S. Gates, K. E. Wise, C. Park, and E. J. Siochi, Compos. Sci. Technol. **63**, 1671 (2003).
[22]T. Hertel, R. E. Walkup, and P. Avouris, Phys. Rev. B **58**, 13870 (1998).
[23]A. Rochefort, P. Avouris, F. Lesage, and D. R. Salhub, Phys. Rev. B **60**, 013824 (1999).
[24]R. S. Ruoff, D. Qian, and W. K. Liu, C. R. Phys. **4**, 993 (2003).
[25]C. Zhu, H. Byrd, and J. Nocedal, ACM Trans. Math. Softw. **23**, 550 (1997).
[26]D. C. Rapaport, *The Art of Molecular Dynamics Simulation*, 1st Ed. (Cambridge University Press, Cambridge, UK, 1995), p.78.
[27]A. R. Leach, *Molecular Modeling Principles and Applications*, 2nd Ed. (Prentice–Hall, England, 2001), p.304.
[28]S. Toxvaerd, Phys. Rev. E **47**, 1 (1993).
[29]H. C. Andersen, J. Chem. Phys. **72**, 2384 (1980).
[30]G. J. Martyana, M. E. Tuckerman, D. J. Tobias, and M. L. Klein, Mol. Phys. **87**, 1117 (1996).
[31]H. J. C. Berendsen, J. P. M. Postma, W. F. van Gunsteren, A. DiNola, and J. R. Hauk, J. Chem. Phys. **81**, 3684 (1984).
[32]W. C. Swope, H. C. Anderson, P. H. Berens, and K. R. Wilson, J. Chem. Phys. **76**, 637 (1982).
[33]P. Ren and J. W. Ponder, J. Phys. Chem. B **107**, 5933 (2003).
[34]M. J. Dudek and J. W. Ponder, J. Comput. Chem. **16**, 791 (1995).
[35]O. Gulseren, T. Yildirim, and S. Ciraci, Phys. Rev. B **65**, 153405 (2002).